

# Observational Constraints on Composite Inflationary Models

Phongpichit Channuie<sup>†</sup> and Khamphée Karwan<sup>‡</sup>

<sup>†</sup>*School of Science, Walailak University, 222 Thaiburi, Thasala District, Nakhon Si Thammarat, 80161, Thailand*

<sup>‡</sup>*The Institute for Fundamental Study, Naresuan University, Phitsanulok 65000, Thailand and Thailand Center of Excellence in Physics, Ministry of Education, Bangkok 10400, Thailand*

E-mail: [phongpichit.ch@wu.ac.th](mailto:phongpichit.ch@wu.ac.th), [khampheek@nu.ac.th](mailto:khampheek@nu.ac.th)

**Abstract.** In the light of Planck data, we examine observational constraints on single-field inflation in which the inflaton is a composite field stemming from a four-dimensional strongly interacting field theory. We derive the power spectrum of the curvature perturbations associated to the composite inflationary models based on the non-minimally coupled composite field to gravity. In the case of a composite model inspired by the minimal walking technicolor theory, we find for a large non-minimal coupling,  $\xi$ , limit that the spectrum index depends solely on the number of e-foldings  $\mathcal{N}$ , and a ratio of the inflaton self-coupling  $\kappa$  to  $\xi^2$  is of the order of  $10^6$ , while  $\kappa > 10^{-14}$  for  $\mathcal{N} \sim 55$  in a small  $\xi$  limit. In the case of a glueball model, the confining scale  $\Lambda$  is weakly constrained and the coupling  $\xi$  is found to be large than  $3.5 \times 10^4$  in order to satisfy the observational bound of the power spectrum amplitude and the spectral index at  $2\sigma(\text{CL})$ . However, for a super Yang-Mills one, we discover that the coupling  $\xi$  is constrained to be approximately larger than  $5.0 \times 10^4$  and the scale  $\Lambda$  is constrained to be not less than  $10^{-5}$  in order to satisfy the observational bound of the power spectrum amplitude and the spectral index at  $2\sigma(\text{CL})$ .

**Keywords:** inflation, particle physics - cosmology connection, physics of the early universe

**ArXiv ePrint:** [1307.2880](https://arxiv.org/abs/1307.2880)

---

## Contents

<b>1</b>	<b>Introduction</b>	<b>1</b>
<b>2</b>	<b>Composite Formulations and Background Evolutions</b>	<b>2</b>
<b>3</b>	<b>Power Spectrum and Spectral Index</b>	<b>4</b>
<b>4</b>	<b>Contact with Observations</b>	<b>7</b>
4.1	Techni-Inflation (TI)	7
4.2	Dilatonic/Glueball Inflation (GI)	11
4.3	Super Yang-Mills Inflation (SYMI)	15
<b>5</b>	<b>Conclusions</b>	<b>19</b>

---

## 1 Introduction

It was widely expected that there was a period of accelerating expansion in the very early universe. Such period is traditionally known as inflation. The inflationary paradigm [1–5] tends to solve important issues, e.g. the magnetic monopoles, the flatness, and the horizon problems, plagued the standard big bang theory and successfully describes the generation and evolution of the observed large-scale structures of the universe. The inflationary scenario is formulated so far by the introduction of (elementary) scalar fields (called inflaton) with a nearly flat potential (see, e.g. [6–11]).<sup>1</sup> In general, however, the inflaton need not be an elementary degree of freedom. Recent investigations show that it is possible to construct models in which the inflaton emerges as a composite state of a four-dimensional strongly coupled theory [12–14]. These types of models have already been stamped to be composite inflation<sup>2</sup>.

Practically, all speculative ideas concerning physics of very early universe can be falsified by using the observation of the large scale structure. In particular, the temperature fluctuations observed in the Cosmic Microwave Background (CMB) is basically regarded as providing a clear window to probe the inflationary cosmology. To testify all inflationary models, we need observables including: (i) the scalar spectral index  $n_s$ , (ii) the amplitude of the power spectrum for the curvature perturbations, (iii) tensor-to-scalar ratio  $r$ , (iv) the non-gaussianity parameter  $f_{\text{NL}}$ . Yet, other relevant parameters are the running of scalar spectral index  $\alpha \equiv dn_s/d \ln k$  and the spectral index for tensor perturbations  $n_T$ . Most recently, the Planck satellite data showed that the spectral index  $n_s$  of curvature perturbations is constrained to be  $n_s = 0.9603 \pm 0.0073$  and ruled out the exact scale-invariance ( $n_s = 1$ ) at more than  $5\sigma$  confident level (CL), whilst the amplitude of the power spectrum for the curvature perturbations  $|\zeta|^2$  is bounded to be  $\mathcal{A}_s = 3.089_{-0.027}^{+0.024}$  [15] with  $\mathcal{A}_s \equiv \ln (|\zeta|^2 \times 10^{10})$ .

In this work, we compute the power spectrum for the primordial curvature perturbations generated in various composite inflationary models. Then we constrain the power spectrum

---

<sup>1</sup>However, the theories featuring elementary scalar fields are unnatural meaning that quantum corrections generate unprotected quadratic divergences which must be fine-tuned away. Therefore, it would be of great interest to imagine natural models underlying the cosmic inflation.

<sup>2</sup>There were other models of super or holographic composite inflation[26–33].

using the observational bound for  $n_s$  and  $\mathcal{A}_s$  from the Planck data. The paper is organized as follows: In section (2), we first spell out the setup for generic model of composite paradigm. We then derive equations of motion and useful expressions. In section (3), we calculate the power spectrum of the primordial curvature perturbations by supposing that the potential energy of the inflaton dominates the kinetic energy and the slow-roll parameter is nearly constant. In section (4), the spectral index and power spectrum amplitude for various composite inflation models are examined, and the range of the model parameters in which these quantities satisfy the observational bound is estimated. Finally, the conclusions are given in section (5).

## 2 Composite Formulations and Background Evolutions

Recently, it has already been shown that cosmic inflation can be driven by four-dimensional strongly interacting theories non-minimally coupled to gravity [12–14]. The general action for composite inflation in the Jordan frame takes the form for scalar-tensor theory of gravity as <sup>3</sup>

$$\mathcal{S}_{\text{CI,J}} = \int d^4x \sqrt{-g} \left[ \frac{M_{\text{P}}^2}{2} F(\Phi) R - \frac{1}{2} G(\Phi) g^{\mu\nu} \partial_\mu \Phi \partial_\nu \Phi - V(\Phi) \right]. \quad (2.1)$$

The functions  $F(\Phi)$  and  $G(\Phi)$  in this action are defined as

$$F(\Phi) = 1 + \frac{\xi}{M_{\text{P}}^2} \Phi^{\frac{2}{d}} \quad \text{and} \quad G(\Phi) = \Phi^{\frac{2-2d}{d}}, \quad (2.2)$$

where  $d$  is the mass dimension of the composite field  $\Phi$ . The non-minimal coupling to gravity is signified by the dimensionless coupling  $\xi$ . Here, we write the general action for the composite inflation in the form of scalar-tensor theory of gravity in which the inflaton non-minimally couples to gravity. The importance of this decision resides in the fact that the non-minimal coupling between inflaton and gravity is required for some models of composite inflation to satisfy the observations.

Let us next derive the equations of motion describing the background evolution. According to the above action, the Friedmann equation and the evolution equations for the background field are respectively given by

$$3M_{\text{P}}^2 F H^2 + 3M_{\text{P}}^2 \dot{F} H = 3M_{\text{P}}^2 H^2 F (1 + 2\mathcal{F}_t) = \frac{1}{2} G \dot{\Phi}^2 + V(\Phi), \quad (2.3)$$

$$3M_{\text{P}}^2 F H^2 + 2M_{\text{P}}^2 \dot{F} H + 2M_{\text{P}}^2 F \dot{H} + 2M_{\text{P}}^2 \ddot{F} = -\frac{1}{2} G \dot{\Phi}^2 + V(\Phi), \quad (2.4)$$

$$G \ddot{\Phi} + 3HG\dot{\Phi} + \frac{1}{2} G_\Phi \dot{\Phi}^2 + V_\Phi = 3M_{\text{P}}^2 F_\Phi (\dot{H} + 2H^2), \quad (2.5)$$

where  $\mathcal{F}_t = \dot{F}/(2HF)$ ,  $H$  is the Hubble parameter, subscripts “ $\Phi$ ” denote derivative with respect to  $\Phi$ , and the dot represents derivative with respect to time,  $t$ . In order to derive the slow-roll parameter  $\epsilon$ , we consider the combination (eq.(2.4) – eq.(2.3)) /  $M_{\text{P}}^2 H^2 F$  which yields

$$-\frac{\dot{H}}{H^2} = -\mathcal{F}_t + \frac{G\dot{\Phi}^2}{2H^2 M_{\text{P}}^2 F} + \frac{F_{\Phi\Phi} \dot{\Phi}^2}{2H^2 F} + \frac{F_\Phi \ddot{\Phi}}{2H^2 F} = \epsilon, \quad \mathcal{F}_t = \frac{\dot{F}}{2HF} = \frac{F_\Phi \dot{\Phi}}{2HF}. \quad (2.6)$$

---

<sup>3</sup>We used the signature of the matrix as  $(-, +, +, +)$  throughout the paper.

For convenience, we will set  $M_{\text{p}}^2 = 1$  in the following calculations. During inflation, we suppose that the inflaton field  $\Phi$  is slowly evolving such that  $V(\Phi) \gg G(\Phi)\dot{\Phi}^2/2$ . Consequently, we can write the Friedmann equation and the evolution equation for the field  $\Phi$  as

$$3H^2F(1 + 2\mathcal{F}_t) = V(\Phi), \quad (2.7)$$

$$\Phi' = \frac{F_\Phi}{G}(2 - \epsilon) - \frac{V_\Phi}{3GH^2}, \quad (2.8)$$

where a prime denote a derivative with respect to  $\mathcal{N} = \ln a$  and  $a$  is the cosmic scale factor. Eq. (2.8) suggests that  $|\ddot{\Phi}| \ll H|\dot{\Phi}|$  during inflation, so that we can neglect  $\ddot{\Phi}$  in eq. (2.6) and hence we get

$$\epsilon = -\mathcal{F}_t + \frac{G\dot{\Phi}^2}{2H^2F} + \frac{F_{\Phi\Phi}\dot{\Phi}^2}{2H^2F}. \quad (2.9)$$

Substituting  $\epsilon$  from this equation in to eq. (2.8) and using eq. (2.7), we get

$$\Phi' = \frac{-2\mathcal{Y}FF_\Phi + F_\Phi^2 + \sqrt{(F_\Phi^2 - 2F(\mathcal{Y}F_\Phi + G))^2 - 8FF_\Phi(F_{\Phi\Phi} + G)(\mathcal{Y}F - 2F_\Phi) - 2FG}}{2F_\Phi(F_{\Phi\Phi} + G)}, \quad (2.10)$$

where  $\mathcal{Y} = V_\Phi/V$ . We will show in section (4) that this equation fits well with full numerical integration. Substituting  $\Phi'$  back into eq. (2.9), we get

$$\begin{aligned} \epsilon = - & \left[ -2\mathcal{Y}FGF_\Phi - 3GF_\Phi^2 - 2\mathcal{Y}^2FF_\Phi^2 + \mathcal{Y}F_\Phi^3 + 2\mathcal{Y}FF_\Phi F_{\Phi\Phi} - 4F_\Phi^2 F_{\Phi\Phi} - 2FG^2 + \right. \\ & \mathcal{Y}F_\Phi \sqrt{(F_\Phi^2 - 2F(\mathcal{Y}F_\Phi + G))^2 - 8FF_\Phi(F_{\Phi\Phi} + G)(\mathcal{Y}F - 2F_\Phi) +} \\ & \left. G\sqrt{(F_\Phi^2 - 2F(\mathcal{Y}F_\Phi + G))^2 - 8FF_\Phi(F_{\Phi\Phi} + G)(\mathcal{Y}F - 2F_\Phi)} \right] [2F_\Phi^2(F_{\Phi\Phi} + G)]^{-1}. \end{aligned} \quad (2.11)$$

To compute the number of e-foldings of inflation, the priority is to determine the expression for the field  $\Phi$  at the end of inflation. Without any approximation, we can use eqs. (2.6) and (2.5) to write  $\epsilon$  in terms of  $\Phi$  and  $\Phi'$  as

$$\epsilon = \frac{-F_\Phi \left( 6F_\Phi (\mathcal{Y}\Phi' - 2) + 6\mathcal{Y}F + (\Phi')^2 G_\Phi \right) + G\Phi' (2\Phi' F_{\Phi\Phi} + F_\Phi (\mathcal{Y}\Phi' - 8)) + 2G^2 (\Phi')^2}{6F_\Phi^2 + 4FG}. \quad (2.12)$$

To obtain the above equation, we have used the Friedmann equation and the evolution equation for  $\Phi$  of the form

$$V(\Phi) = 3H^2F \left( 1 + 2\mathcal{F}_t - \frac{G\Phi'^2}{2F} \right), \quad (2.13)$$

$$\Phi'' = (\epsilon - 3)\Phi' - \frac{G_\Phi\Phi'^2}{2G} - \frac{V_\Phi}{GH^2} + 3\frac{F_\Phi}{G}(2 - \epsilon), \quad (2.14)$$

$$\epsilon = -\mathcal{F}_t + \frac{F_{\Phi\Phi}\Phi'^2 + F_\Phi\Phi'' - \epsilon F_\Phi\Phi'}{2F} + \frac{G\Phi'^2}{2F}. \quad (2.15)$$

We can determine the relation between  $\Phi$  and  $\Phi'$  when inflation ends. From eq. (2.12), we set  $\epsilon = 1$  to yield

$$\Phi' = \frac{\sqrt{(8GF_\Phi + 6\mathcal{Y}F_\Phi^2)^2 + 8(F(3\mathcal{Y}F_\Phi + 2G) - 3F_\Phi^2)(-F_\Phi G_\Phi + G(2F_{\Phi\Phi} + \mathcal{Y}F_\Phi) + 2G^2)}}{2F_\Phi G_\Phi - 2G(2F_{\Phi\Phi} + \mathcal{Y}F_\Phi) - 4G^2} + \frac{4GF_\Phi + 3\mathcal{Y}F_\Phi^2}{-F_\Phi G_\Phi + G(2F_{\Phi\Phi} + \mathcal{Y}F_\Phi) + 2G^2}. \quad (2.16)$$

This relation should satisfy the evolution equation (2.14), so that we substitute this relation into eq. (2.14) by using  $\Phi'' = \Phi' d\Phi'/d\Phi$  and setting  $\epsilon = 1$ . As a result, we get an algebraic equation for  $\Phi$  at the end of inflation. In general, it is complicated to solve the equation for  $\Phi$  analytically. However, for our convenience, we will perform our calculation using the field variable  $\varphi$  with canonical dimension for which  $F = 1 + f\xi\varphi^2$  and  $G = g_0$ , where  $f$  and  $g_0$  are constant. In terms of field  $\varphi$ , the algebraic equation for the field can be solved analytically if one considers simple potentials such as  $V(\varphi) \propto \varphi^4$ , etc.

In the case of a complicated form of the potentials in which the equation for the field at the end of inflation cannot be solved analytically, we estimate, instead, the expression for the field by making an expansion for large and small  $\xi$  respectively as

$$0 = \frac{\varphi(\mathcal{X}^2 - 8\mathcal{X} + 4)}{2\mathcal{X}^2} + \frac{g_0\varphi^2(\mathcal{X}^4 - 22\mathcal{X}^3 + 96\mathcal{X}^2 - 88\mathcal{X} + 16) + 12(\mathcal{X} - 2)\mathcal{X}^3}{24f\varphi\mathcal{X}^4\xi} + \mathcal{O}(1/\xi^2), \quad (2.17)$$

and

$$0 = \frac{2\mathcal{X}}{g_0\varphi} - \frac{2\sqrt{2}}{\sqrt{g_0}} - \frac{f\xi(\sqrt{2}g_0^{3/2}\varphi^3 - 2g_0\varphi^2(\mathcal{X} + 2) + 2\sqrt{2}\sqrt{g_0}\varphi(2\mathcal{X} + 1) + 2(\mathcal{X} - 1)\mathcal{X})}{g_0^2\varphi} + \mathcal{O}(\xi^2), \quad (2.18)$$

where  $\mathcal{X} = \varphi\mathcal{Y}$  is either constant or non-polynomial function of  $\varphi$ , e. g.,  $\mathcal{X} = 4$  for  $V \propto \varphi^4$ . Here, however, the equation for the field at the end of inflation is cumbersome to write down explicitly. Having computed the field  $\Phi$  at the end of inflation, one can determine the number of e-foldings via

$$\mathcal{N}(\Phi) = \ln \frac{a_e}{a} = \int_a^{a_e} \frac{1}{\tilde{a}} d\tilde{a} = \int_t^{t_e} H d\tilde{t} = \int_\Phi^{\Phi_e} \frac{H}{\dot{\Phi}} d\tilde{\Phi} = \int_\Phi^{\Phi_e} \frac{1}{\dot{\Phi}'} d\tilde{\Phi}, \quad (2.19)$$

where the subscript “e” denotes the evaluation at the end of inflation and  $\Phi'$  is given by eq. (2.10). At the observable perturbation exits the horizon, we can evaluate the field  $\Phi$  once the number of e-foldings  $\mathcal{N}$  is known. Determining the value of  $\Phi$  and  $\Phi'$  when the perturbations exit the horizon allows us to compute the spectral index and power spectrum amplitude for the curvature perturbations in the next sections.

### 3 Power Spectrum and Spectral Index

In order to compute the power spectrum for the curvature perturbations, we suppose that  $\mathcal{F}_t$  and  $\epsilon$  are approximately constant during the time at which the perturbations exit the

horizon. Supposing that  $\epsilon$  is approximately constant, one can show that [17]

$$a = -\frac{1}{H\tau(1-\epsilon)}, \quad \frac{d^2a}{a d\tau^2} = \frac{2-\epsilon}{\tau^2(1-\epsilon)^2}, \quad (3.1)$$

where  $\tau = \int dt/a$  is the conformal time. When  $\mathcal{F}_t$  and  $\epsilon$  are nearly constant, the second order action for the curvature perturbation in the scalar-tensor theory [18, 19] takes the form

$$S_2 = \int d\tau d^3k a^2 F \left\{ \left( \frac{3\mathcal{F}_t^2}{(1+\mathcal{F}_t)^2} + \frac{G\dot{\Phi}^2}{2H^2 F (1+\mathcal{F}_t)^2} \right) \left( \frac{d\zeta_k(\tau)}{d\tau} \right)^2 + k^2 \frac{\mathcal{F}_t + \epsilon}{1+\mathcal{F}_t} \zeta_k^2(\tau) \right\}, \quad (3.2)$$

where  $\zeta_k(\tau)$  is the Fourier mode of the curvature perturbation. In terms of the variable  $v_k(\tau) \equiv z\zeta_k(\tau)$ , where

$$z \equiv a \sqrt{3F \frac{\mathcal{F}_t^2}{(1+\mathcal{F}_t)^2} + \frac{G\dot{\Phi}^2}{2H^2(1+\mathcal{F}_t)^2}}, \quad (3.3)$$

the action (3.2) becomes

$$\begin{aligned} S_2 &= \int d\tau d^3k \left\{ \left( \frac{dv_k(\tau)}{d\tau} \right)^2 + c_s^2 k^2 v_k^2(\tau) + z^{-1} \frac{d^2 z}{d\tau^2} v_k^2(\tau) \right\}, \\ &= \int d\tau d^3k \left\{ \left( \frac{dv_k(\tau)}{d\tau} \right)^2 + c_s^2 k^2 v_k^2(\tau) + \frac{1}{\tau^2} \left( \mu^2 - \frac{1}{4} \right) v_k^2(\tau) \right\}. \end{aligned} \quad (3.4)$$

Here,

$$c_s^2 = (\mathcal{F}_t + \epsilon) (1 + \mathcal{F}_t) \left[ 3\mathcal{F}_t^2 + \frac{G\dot{\Phi}^2}{2H^2 F} \right]^{-1}, \quad (3.5)$$

$$\mu = \sqrt{\frac{9}{4} + 3\epsilon + 3\mathcal{F}_t + 10\epsilon^2 + 5\epsilon\mathcal{F}_t + \mathcal{F}_t^2} + \mathcal{O}(\epsilon^3) \simeq \frac{3}{2} + \epsilon + \mathcal{F}_t + \mathcal{O}(\epsilon^2). \quad (3.6)$$

Since  $\mathcal{F}_t$  and  $\epsilon$  are approximated to be constant in our calculation,  $c_s$  and  $\mu$  are presumably constant. The evolution equation from the action (3.4) is

$$\frac{d^2 v_k}{d\tau^2} + \left[ c_s^2 k^2 - \frac{1}{\tau^2} \left( \mu^2 - \frac{1}{4} \right) \right] v_k = 0. \quad (3.7)$$

The solutions of this equation can be written as

$$v_k(\tau) = \sqrt{c_s k |\tau|} \left( c_1 H_\mu^{(1)}(c_s k |\tau|) + c_2 H_\mu^{(2)}(c_s k |\tau|) \right), \quad (3.8)$$

where  $c_1$  and  $c_2$  are the integration constant, and  $H_\mu^{(1)}$  and  $H_\mu^{(2)}$  are the Hankal functions of the first and second kind respectively. Using the asymptotic expression for the Hankal function,

$$H_\mu^{(1)}(x \gg 1) \sim \sqrt{\frac{2}{\pi x}} e^{i(x - \frac{\pi}{2}\mu - \frac{\pi}{4})}, \quad H_\mu^{(2)}(x \gg 1) \sim \sqrt{\frac{2}{\pi x}} e^{-i(x - \frac{\pi}{2}\mu - \frac{\pi}{4})}, \quad (3.9)$$

the solution on the sub-horizon scale ( $c_s k |\tau| \gg 1$ ) becomes

$$v_k = c_1 \sqrt{\frac{2}{\pi}} e^{i(c_s k |\tau| - \frac{\pi}{2}\mu - \frac{\pi}{4})}, \quad (3.10)$$

where we have neglected  $e^{-i c_s k |\tau|}$ . On sub-horizon scales, the first term in the square bracket of eq. (3.7) is much larger than the second one, so that the solution on the sub-horizon scale takes the plane-wave form [17, 18]:

$$v_k \simeq \frac{e^{i c_s k |\tau|}}{\sqrt{2 c_s k}}. \quad (3.11)$$

Matching this plane-wave solution to eq. (3.10), we get

$$c_1 = \sqrt{\frac{\pi}{4 c_s k}} e^{-i(\frac{\pi}{2}\mu + \frac{\pi}{4})}. \quad (3.12)$$

Using the asymptotic behavior for the Hankal function,

$$H_\mu^{(1)}(x \ll 1) \sim \sqrt{\frac{2}{\pi}} e^{-i\frac{\pi}{2}} 2^{\mu-\frac{3}{2}} \frac{\Gamma(\mu)}{\Gamma(3/2)} x^{-\mu}, \quad (3.13)$$

and the above expression for  $c_1$ , we can write the solution on superhorizon scale as

$$|v_k|^2 = \frac{1}{2 c_s k} 2^{2\mu-3} \left( \frac{\Gamma(\mu)}{\Gamma(3/2)} \right)^2 (c_s k |\tau|)^{-2\mu+1}. \quad (3.14)$$

Using this result, the power spectrum for the curvature perturbation is obtained as

$$\mathcal{P}_\zeta = \frac{k^3}{2\pi^2} |\zeta|^2 = \frac{k^3}{2\pi^2} \frac{|v_k|^2}{z^2} \simeq \frac{H^2 (1 + \mathcal{F}_t)^2}{8\pi^2 F c_s^3 (3\mathcal{F}_t^2 + G\Phi'^2/2F)} (c_s k |\tau|)^{-2\mu+3}. \quad (3.15)$$

At the horizon exit  $c_s k |\tau| = 1$ , the expression for the power spectrum becomes

$$\mathcal{P}_\zeta \simeq \frac{(1 + \mathcal{F}_t)^{1/2} (3\mathcal{F}_t^2 + G\Phi'^2/2F)^{1/2} H^2}{F (\epsilon + \mathcal{F}_t)^{3/2}} \Big|_{c_s k |\tau|=1} \frac{1}{8\pi^2}. \quad (3.16)$$

The spectrum index for this power spectrum can be computed via

$$n_s = \frac{d \ln \mathcal{P}_\zeta}{d \ln k} + 1 \simeq \frac{1}{H} \frac{d \ln \mathcal{P}}{dt} + 1 \simeq 1 - 2\epsilon - 2\mathcal{F}_t + \delta_\Phi, \quad (3.17)$$

where

$$\delta_\Phi \equiv \frac{\Phi'}{2} \frac{d \ln [G\Phi'^2 / (2F + 3\mathcal{F}_t^2)]}{d\Phi} + \frac{3\Phi'}{2} \frac{d \ln [\epsilon + \mathcal{F}_t]}{d\Phi}. \quad (3.18)$$

The amplitude of the curvature perturbation can be directly read from the power spectrum as

$$|\zeta|^2 \simeq \frac{(1 + \mathcal{F}_t)^{1/2} (3\mathcal{F}_t^2 + G\Phi'^2/2F)^{1/2} V}{24\pi^2 F^2 (\epsilon + \mathcal{F}_t)^{3/2} (1 + 2\mathcal{F}_t)} \Big|_{c_s k |\tau|=1}, \quad (3.19)$$

where we have used eq. (2.7) to write  $H^2$  in terms of  $V$ . When  $\mathcal{F}_t$  is approximately constant, and  $\Phi$  is slowly rolling, the expression for  $\epsilon$  can be obtained by differentiating eq. (2.7) with respect to time. The result is

$$\epsilon = \mathcal{F}_t - \frac{V_\Phi}{V} \frac{F}{F_\Phi} \mathcal{F}_t. \quad (3.20)$$

The evolution equation (2.10) will be simplified if we add the approximations  $\mathcal{F}_t \sim \text{constant}$  and  $\epsilon \sim \text{constant}$ . Imposing the conditions  $G\dot{\Phi}^2/2 \ll V$ ,  $\mathcal{F}_t \sim \text{constant}$  and  $\epsilon \sim \text{constant}$  and using  $\epsilon$  from eq. (3.20), eq. (2.5) becomes

$$\Phi' = \left( 2\frac{F_\Phi}{G} - \frac{V_\Phi F}{V G} \right) \left[ 1 + \frac{V_\Phi F_\Phi}{V G} + \frac{F_\Phi^2}{2FG} - \frac{V_\Phi F_\Phi}{V 2G} \right]^{-1}. \quad (3.21)$$

In the next section, we will examine  $n_s$  and  $|\zeta|^2$  both analytically and numerically. For the analytical calculation, we write  $n_s$  and  $|\zeta|^2$  in terms of  $\Phi$  at the horizon exit using eqs. (3.20) and (3.21). It is worthy noting that the power spectrum is obtained by supposing that  $\mathcal{F}_t$  and  $\epsilon$  are constant. Here it is more calculable for our investigations to impose  $\Phi'$  given in eq.(3.20) and  $\epsilon$  in eq(3.21) since the obtained expressions,  $n_s$  and  $|\zeta|^2$ , takes simple form, however, reflecting reliable features. Note that for our numerical analysis we will use the expressions  $\Phi'$  given in eq(2.10) for better approximations.

In order to determine  $n_s$  and  $|\zeta|^2$  numerically, we estimate the value of the field  $\Phi$  around the horizon exit from eq. (2.19) by suitably choosing the number of e-foldings  $\mathcal{N}$  before inflation ends. Using this value of  $\Phi$  with eq. (2.10), we determine  $\Phi'$  and  $\mathcal{F}_t$  at the horizon exit. From this  $\mathcal{F}_t$ , we compute  $\epsilon$  from eq. (3.20), and then we compute  $n_s$  and  $|\zeta|^2$  using eqs. (3.17) and (3.19) respectively.

## 4 Contact with Observations

### 4.1 Techni-Inflation (TI)

The authors of [12] recently demonstrated that it is possible to obtain a successful inflation in which the inflaton is a composite field stemming from a four-dimensional strongly interacting field theory. In this work, they engaged the simplest models of technicolor passing precision tests well known as the minimal walking technicolor (MWT) theory [20–23] with the standard (slow-roll) inflationary paradigm as a template for composite inflation. The inflaton identified with the lightest composite state, i.e.  $\Phi \equiv \varphi$ , in which we couple non-minimally to gravity. The resulting action in the Jordan frame is given by [12]:

$$\mathcal{S}_{\text{TI}} = \int d^4x \sqrt{-g} \left[ \frac{1 + \xi\varphi^2}{2} R - \frac{1}{2} g^{\mu\nu} \partial_\mu \varphi \partial_\nu \varphi - V_{\text{TI}}(\varphi) \right], \quad (4.1)$$

where

$$V_{\text{TI}}(\varphi) = -\frac{m^2}{2}\varphi^2 + \frac{\kappa}{4}\varphi^4, \quad (4.2)$$

in which  $\kappa$  is a self coupling and the inflaton mass is  $m_{\text{TI}}^2 = 2m^2$ . Since  $m_{\text{TI}}$  is order of the GeV energy scale,  $\kappa$  should be order of unity and  $\Phi$  during inflation is order of Planck mass, we neglect  $m_{\text{TI}}^2$  term in our calculation. For this model, we have

$$F(\varphi) = 1 + \xi\varphi^2 \quad \text{and} \quad G = 1. \quad (4.3)$$

Before computing  $n_s$  and  $|\zeta|^2$  for this composite inflation model, let us check the validity of our slow-roll approximation. The differences among the solutions for the full evolution equation



for the field eq. (2.14), the evolution equation for the field in slow-roll limit eqs. (2.10) and (3.21) are quantified by a fraction

$$\Delta = \left| \frac{\varphi_j - \varphi_k}{\varphi_j} \right|, \quad (4.4)$$

where  $\varphi_j$  and  $\varphi_k$  are the numerical solutions for eqs. (2.14), (2.10) or (3.21).

In our numerical integration, the initial conditions for  $\varphi_i$  and  $\varphi'_i$  at  $a = a_i$  are set to be for those at the horizon exit. Using these initial conditions for  $\varphi$  and  $\varphi'$ , we solve eq. (2.14), (2.10) and (3.21) numerically and plot  $\Delta$  in figure (1). Moreover, we use the numerical solution for eq. (2.14) to plot  $\mathcal{F}_t$  and  $\epsilon$  if figure (2), where  $\epsilon$  is computed from eq. (2.15).

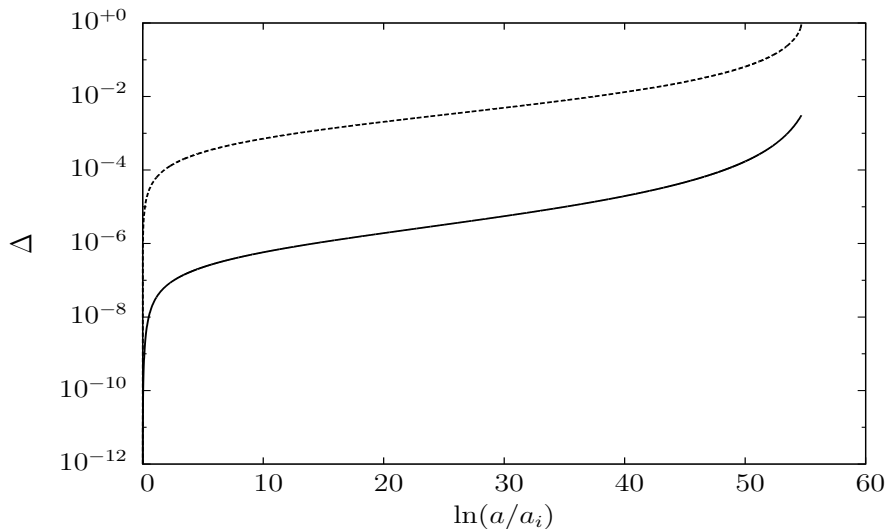


**Figure 1.** The solid line represents the difference between the solutions of eq. (2.14) and eq. (2.10), while the long dashed line represents the difference between the solutions of eq. (2.14) and eq. (3.21). In this plot, we set  $\xi = 4.5 \times 10^4$ ,  $\kappa = 1$  and  $\mathcal{N} = 55$ .

Needless to say from figure (1), we see that the solution of eq. (3.21) mimics the solution of eq. (2.14) better than that of eq. (3.21). However, around the horizon exit, eq. (3.21) is a good approximation of eq. (2.14). Figure (2) shows that the constancy of  $\mathcal{F}_t$  and  $\epsilon$  during initial state of inflation, and the relevant expressions for eq. (2.19) are a good approximation.

For this form of the potential, eqs. (3.17) and (3.19) yield

$$n_s = 1 - \frac{6\xi}{1 + \varphi^2\xi(1 + 6\xi)} + \frac{4 + 4\xi(4 + \varphi^2)}{3[\varphi + 4\xi\varphi + \varphi^3\xi(1 + 6\xi)]^2} - \frac{76 + 30\xi\varphi^2}{3\varphi^2[1 + \xi(4 + \varphi^2(1 + 6\xi))]}, \quad (4.5)$$

and

$$|\zeta|^2 = \frac{\kappa\varphi^6(6\varphi^2\xi^2 + (\varphi^2 + 4)\xi + 1)(\varphi^2\xi(6\xi + 1) + 1)}{768(\pi\varphi^2\xi + \pi)^2(6\varphi^2\xi^2 + (\varphi^2 - 4)\xi + 1)}, \quad (4.6)$$

where  $\varphi$  is evaluated at the horizon exit. From eq. (4.5), we see that  $n_s$  depends on the parameter  $\xi$ . When  $\xi \rightarrow 0$ , we have

$$n_s \simeq \left(1 - \frac{24}{\varphi^2}\right) + \left(\frac{96}{\varphi^2} + 8\right)\xi + \mathcal{O}(\xi^2), \quad (4.7)$$

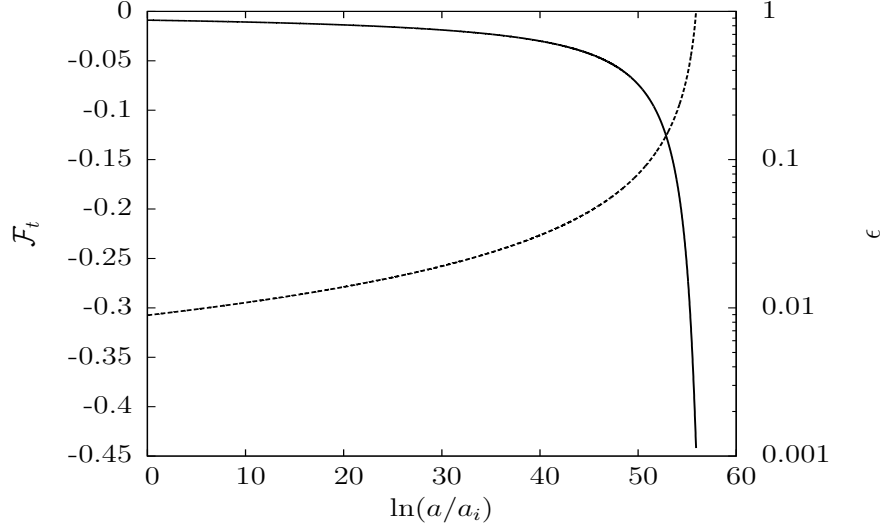


**Figure 2.** The evolution of  $\mathcal{F}_t$  is represented by solid line, while the evolution of  $\epsilon$  is represented by long dashed line. In this plot, we set  $\xi = 4.5 \times 10^4$ ,  $\kappa = 1$  and  $\mathcal{N} = 55$ .

and when  $\xi \rightarrow \infty$ , we get

$$n_s \simeq 1 - \frac{8}{3\varphi^2\xi} + \frac{4(-7 + \varphi^2)}{9\varphi^4\xi^2} + \mathcal{O}(1/\xi^3). \quad (4.8)$$

The value of the field  $\varphi$  at the horizon exit has to lie within a suitable range, such that the slow-roll evolution of the field  $\varphi$  or equivalently inflation lasts sufficiently long. Hence, possible ranges of  $\varphi$  can be estimated from eq. (2.10). When  $\xi \rightarrow 0$  and  $\xi \rightarrow \infty$ , eq. (2.10) respectively yields

$$\frac{\varphi'}{\varphi} \simeq -\frac{4}{\varphi^2} + \frac{16}{\varphi^2}\xi + \mathcal{O}(\xi^2), \quad \text{and} \quad \frac{\varphi'}{\varphi} \simeq -\frac{2}{3\varphi^2\xi} + \mathcal{O}(1/\xi^2). \quad (4.9)$$

From these equations, we see that when  $\xi$  is large, the slow-roll evolution of the field requires  $2/(3\varphi^2\xi) \ll 1$ . Hence, eq. (4.8) gives  $n_s \sim 1 - 4(\varphi'/\varphi)$ , implying that  $n_s$  can significantly deviate from unity if  $\varphi'/\varphi \gtrsim 0.001$ . In this case, the dominant contributions to  $\mathcal{N}$  yield  $4\mathcal{N} \simeq 3\varphi^2\xi - 3\varphi_e^2\xi$  with  $\varphi_e^2 \simeq 2/(3\xi)$ . Hence we find that  $\varphi^2\xi \sim 4\mathcal{N}/3 + 2/3$ . Using eq. (4.8), one gets  $n_s \simeq 1 - 4/(2\mathcal{N} + 1)$ .

Apparently, the dominant contributions to  $n_s$  depend only on the number of e-foldings. Besides, we discover that the observational bound on  $n_s$  cannot be used to constrain  $\kappa$  and  $\xi$ . Using the observational bound on the power spectrum amplitude, however, one can put a constraint only on the ratio  $\kappa/\xi^2$  but neither on  $\kappa$  nor  $\xi$ . This is so since for large  $\xi$  the power spectrum amplitude takes the form

$$\begin{aligned} |\zeta|^2 &\simeq \frac{\kappa\varphi^4}{128\pi^2} + \frac{\kappa\varphi^2(\varphi^2 - 4)}{768\pi^2\xi} + \mathcal{O}(1/\xi^2) \\ &\sim \frac{\kappa\mathcal{N}(2\mathcal{N} + 1)}{144\pi^2\xi^2} + \mathcal{O}(1/\xi^3). \end{aligned} \quad (4.10)$$

This equation shows that at leading order, the power spectrum amplitude depends on the number of e-foldings and the ratio  $\kappa/\xi^2$ . From the numerical calculation, we get the viable

range of the number of e-foldings  $43 \lesssim \mathcal{N} \lesssim 62$  for  $n_s = 0.96 \pm 0.007$ . From the viable range of e-foldings, we can get  $3.04 \lesssim \mathcal{A}_s \lesssim 3.13$  if  $3.9 \times 10^6 < \kappa/\xi^2 < 8.9 \times 10^6$  for  $\mathcal{N} \simeq 55$ . We evidently see from the figure (3) together with figure (4) that  $\kappa$  is possibly constrained to be order of unity for  $\xi \sim 10^4$ . Nevertheless, these results are valid only for large  $\xi$ . For the

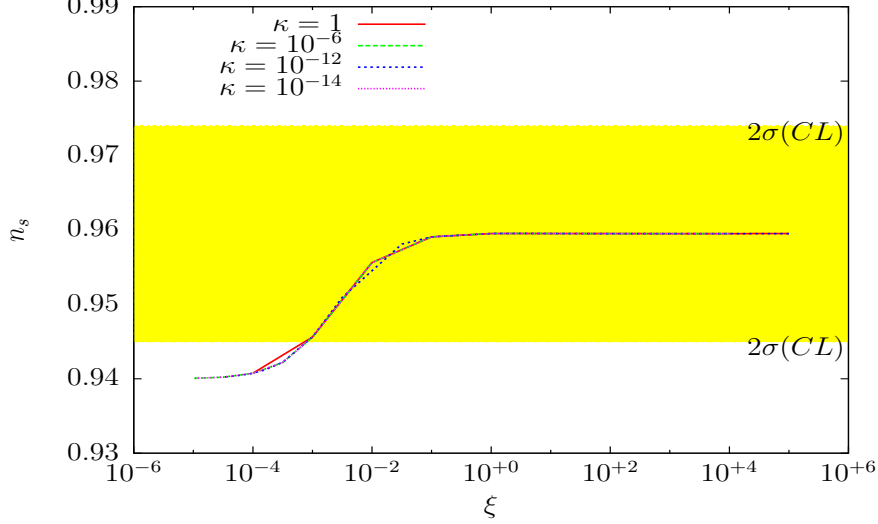


**Figure 3.** The spectral index as a function of  $\kappa$  and  $\xi$  for  $\mathcal{N} \simeq 55$ . The yellow band corresponds to the  $\pm 2\sigma$  uncertainty.

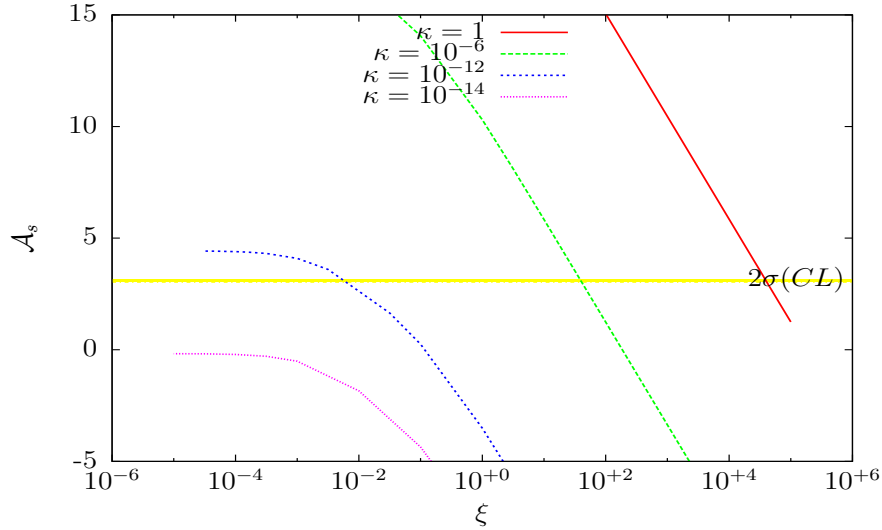


**Figure 4.** The amplitude of power spectrum as a function of  $\kappa$  and  $\xi$  for  $\mathcal{N} \simeq 55$ . The yellow band corresponds to the  $\pm 2\sigma$  uncertainty.

small  $\xi$  case, the situations change as follows. In such case, eq. (4.9) suggests that  $2 \ll \varphi$  when the field is slowly rolling. In this case, it follows from eq. (4.7) that both  $\varphi'/\varphi$  and  $\xi$  can give the contributions to  $n_s$  if their magnitudes are of the same order. It can be shown that the ratio  $\varphi'/\varphi$  is related to the number of e-foldings between the horizon exit and the end of inflation as  $\mathcal{N} \simeq \varphi^2/8 - \varphi_e^2/8 \simeq \varphi^2/8 - 1$  with  $\varphi_e^2 \sim 8$ . Hence, from eq. (4.7), we see that, for a given the number of e-foldings,  $n_s$  decreases when  $\xi$  decreases. When  $\xi$  is small,

we can expand  $|\zeta|^2$  as

$$|\zeta|^2 \simeq \frac{\kappa\varphi^6}{768\pi^2} - \frac{\xi(\kappa\varphi^6(\varphi^2 - 8))}{768\pi^2} + \mathcal{O}(\xi^2) \simeq \frac{2\kappa(\mathcal{N} + 1)^3}{3\pi^2} + \mathcal{O}(\xi). \quad (4.11)$$

This relation shows that the observational bound on the power spectrum amplitude can be used to constrain  $\kappa$  for sufficiently small  $\xi$ . Nevertheless, since  $\varphi^2 \gg 2$  during inflation, the power spectrum amplitude can satisfy the observational bound if  $\kappa \ll 10^{-7}$ , which is much smaller than unity expected from the theory at  $\kappa \sim \mathcal{O}(1)$ . Let us consider for instance for  $\mathcal{N} \sim 55$ . We clearly see from figure (4) that the amplitude of power spectrum is less sensitive to a small coupling  $\xi$ . However if the  $\kappa \lesssim 10^{-14}$ , the power spectrum amplitude cannot be satisfied the lower bound at  $2\sigma$  CL. From figures (3) and (4), we see that  $n_s$  and  $\mathcal{A}_s$  can fit observational bound for a wild range of  $\kappa$  when a suitable  $\xi$  is chosen.

## 4.2 Dilatonic/Glueball Inflation (GI)

The simplest examples of strongly coupled theories are pure Yang-Mills theories featuring only gluonic-type fields. It would be of great interest to investigate inflation using these theories. The authors of [13] demonstrated that it is possible to achieve successful inflation where the inflaton emerges as the lightest glueball field associated to a pure Yang-Mills theory. In this case, the inflaton is the interpolating field describing the lightest glueball. The effective Lagrangian for the lightest glueball state, constrained by the Yang-Mills trace anomaly, non-minimally coupled to gravity in the Jordan frame reads

$$\mathcal{S}_{\text{GI}} = \int d^4x \sqrt{-g} \left[ \frac{1 + \xi\Phi^{1/2}}{2} R - \Phi^{-3/2} g^{\mu\nu} \partial_\mu \Phi \partial_\nu \Phi - V_{\text{GI}}(\Phi) \right], \quad (4.12)$$

where

$$V_{\text{GI}}(\Phi) = \frac{\Phi}{2} \ln \left( \frac{\Phi}{\Lambda^4} \right), \quad (4.13)$$

It is convenient to introduce the field  $\varphi$  possessing unity canonical dimension and related to  $\Phi$  as follows:

$$\Phi = \varphi^4 \quad (4.14)$$

From the above assignment, the action then becomes

$$\mathcal{S}_{\text{GI}} = \int d^4x \sqrt{-g} \left[ \frac{1 + \xi\varphi^2}{2} R - 16g^{\mu\nu} \partial_\mu \varphi \partial_\nu \varphi - V_{\text{GI}}(\varphi) \right], \quad (4.15)$$

where

$$V_{\text{GI}}(\varphi) = 2\varphi^4 \ln \left( \frac{\varphi}{\Lambda} \right), \quad (4.16)$$

which yields

$$F(\varphi) = 1 + \xi\varphi^2 \quad \text{and} \quad G = 32. \quad (4.17)$$

In the following calculation, we will study the evolution of the field  $\varphi$  instead of  $\Phi$ , and then study the power spectrum associated with  $\varphi$ . Using the same method as for the Techni-

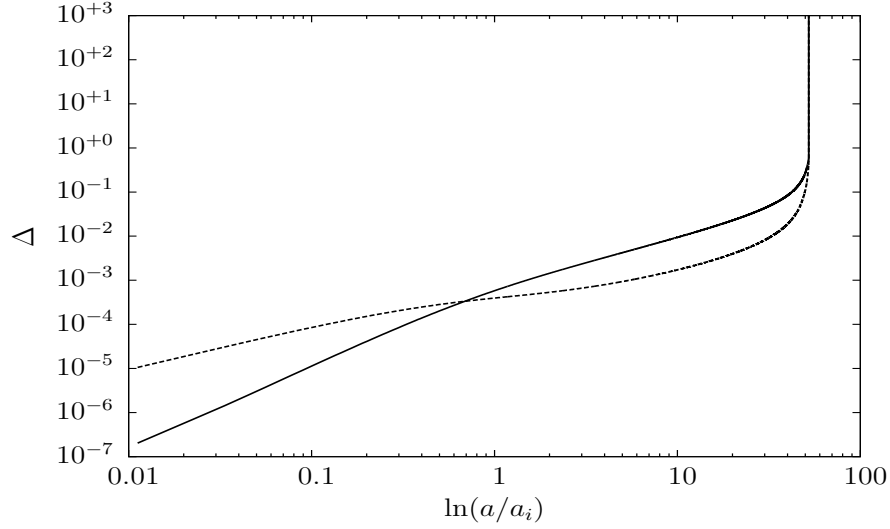


**Figure 5.** The solid line represents the difference between the solutions of eq. (2.14) and eq. (2.10), while the long dashed line represents the difference between the solutions of eq. (2.14) and eq. (3.21). In this plot, we use  $\xi \simeq 10^4$ ,  $\Lambda \simeq 10^{-2}$  and  $\mathcal{N} = 55$ .

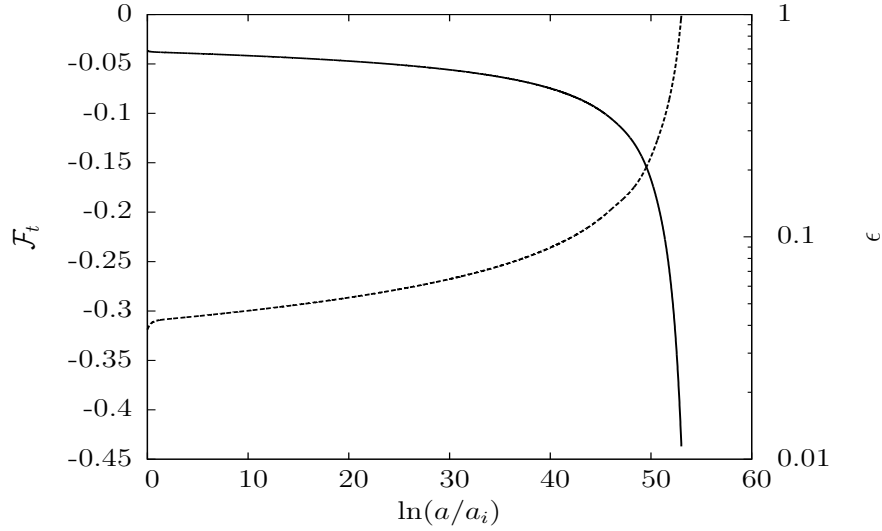


**Figure 6.** The evolution of  $\mathcal{F}_t$  is represented by solid line, while the evolution of  $\epsilon$  is represented by long dashed line. In this plot, we use  $\xi \simeq 10^4$ ,  $\Lambda \simeq 10^{-2}$  and  $\mathcal{N} = 55$ .

Inflation, we plot  $\Delta$ ,  $\mathcal{F}_t$  and  $\epsilon$  in figure (5) and figure (6). From figure (5), we see that for the whole inflation eqs. (2.14) is better approximated by (2.10) rather than (3.21). Similar to the Techni-Inflation, the constancy of  $\mathcal{F}_t$  and  $\epsilon$  and the calculation of e-folding can be validated in figure (6). It is later convenient to introduce a set of parameters:

$$Y \equiv \ln[\varphi/\Lambda], \mathcal{A} \equiv 1 + \xi\varphi^2, \mathcal{B} \equiv \xi\varphi^2(16 + 3\xi), \quad (4.18)$$

$$\mathcal{C} \equiv 832\xi + 54\xi^2 + \mathcal{B} \quad \text{and} \quad \mathcal{D}_{\pm} \equiv 32 + 2(\pm 2\xi + \mathcal{B}). \quad (4.19)$$

For this model of composite inflation, we find

$$n_s \simeq 1 - \left[ 5\varphi \mathcal{A}^3 (16 + \mathcal{B}) + 2Y \left( \mathcal{A}^2 (1536 + \xi (320 + \varphi^2 (3072 + \mathcal{C}) (80 + 21\xi))) \right. \right. \\ \left. \left. + 4Y \left( \mathcal{A} (1280 + \xi (256 + \varphi^2 (2560 + \mathcal{C} (80 + 21\xi))) \right) + 4(768 + \xi (96 + \right. \right. \\ \left. \left. \varphi^2 (2048 + 480\xi + 21\xi^2 + \mathcal{B} (112 + 15\xi + \mathcal{B}))) Y \right) \right) \right] \times \\ \left[ 2\varphi^2 Y (16 + \mathcal{B}) \left( \xi \mathcal{A} + (32 + 4\xi + \mathcal{B}) Y \right)^2 \right]^{-1}, \quad (4.20)$$

and

$$|\zeta|^2 = \frac{\varphi^6 Y^3 (16 + \mathcal{B}) (\xi \mathcal{A} + \mathcal{D}_+ Y)}{3\pi^2 \mathcal{A}^2 (1 + \xi \varphi^2 + 4Y)^2 (-\xi \mathcal{A} + \mathcal{D}_- Y)}. \quad (4.21)$$

One can see from eq. (4.20) that  $n_s$  depends on both  $\xi$  and  $\Lambda$ . In the above expressions,  $\varphi > \Lambda$ . In the small  $\xi$  and large  $\xi$  limits, eq. (4.20) respectively becomes

$$n_s \simeq 1 - \frac{3}{4\varphi^2} - \frac{3}{32\varphi^2 (\ln[\varphi/\Lambda])^2} - \frac{5}{16\varphi^2 \ln[\varphi/\Lambda]} + \left[ \frac{1}{4} + \frac{3}{32\varphi^2} \right. \\ \left. + \frac{7}{2048\varphi^2 (\ln[\varphi/\Lambda])^3} - \frac{3}{32(\ln[\varphi/\Lambda])^2} \right. \\ \left. + \frac{3}{128\varphi^2 (\ln[\varphi/\Lambda])^2} + \frac{1}{16\varphi^2 \ln[\varphi/\Lambda]} \right] \xi + \mathcal{O}(\xi^2), \quad (4.22)$$

and

$$n_s \simeq \frac{-5 - 34 \ln[\varphi/\Lambda] + 24 (\ln[\varphi/\Lambda])^2 + 72 (\ln[\varphi/\Lambda])^3}{2 \ln[\varphi/\Lambda] (1 + 6 \ln[\varphi/\Lambda])^2} \\ + \left[ 2\varphi^2 \ln[\varphi/\Lambda] (1 + 6 \ln[\varphi/\Lambda])^3 \xi \right]^{-1} \left[ -5 - 92 \ln[\varphi/\Lambda] + 128\varphi^2 \ln[\varphi/\Lambda] \right. \\ \left. - 564 (\ln[\varphi/\Lambda])^2 + 1152\varphi^2 (\ln[\varphi/\Lambda])^2 \right. \\ \left. - 1200 (\ln[\varphi/\Lambda])^3 - 1152 (\ln[\varphi/\Lambda])^4 \right]. \quad (4.23)$$

To estimate the magnitude of  $\varphi$  during inflation, we write eq. (2.10) in the small  $\xi$  and large  $\xi$  limits respectively as

$$\frac{\varphi'}{\varphi} \simeq -\frac{4 \ln(\varphi/\Lambda) + 1}{32\varphi^2 \ln(\varphi/\Lambda)} + \xi \frac{1 - 32\varphi^2 \ln(\varphi/\Lambda) + 16 \ln^2(\varphi/\Lambda) + 8 \ln(\varphi/\Lambda)}{1024\varphi^2 \ln^2(\varphi/\Lambda)} + \mathcal{O}(\xi^2) \quad (4.24)$$

$$\frac{\varphi'}{\varphi} \simeq \frac{\sqrt{9 \ln^2(\varphi/\Lambda) + 4 \ln(\varphi/\Lambda) + 1} - 3 \ln(\varphi/\Lambda) - 1}{2 \ln(\varphi/\Lambda)} + \mathcal{O}(1/\xi). \quad (4.25)$$

In the large  $\xi$  limit, eq. (4.25) suggests that the field can slowly evolve when the condition  $\ln(\varphi/\Lambda) \gg 1$  is satisfied. Using the leading contributions to  $\varphi'$  for a large  $\xi$ , we get

$$\mathcal{N} = \mathcal{N}(\varphi) - \mathcal{N}(\varphi_e), \quad (4.26)$$

where

$$54\mathcal{N}(\varphi) \equiv 81 (\ln[\varphi/\Lambda])^2 + 3 (9 \ln[\varphi/\Lambda] + 2) \sqrt{9 (\ln[\varphi/\Lambda])^2 + 4 \ln[\varphi/\Lambda] + 1} \\ + 54 \ln[\varphi/\Lambda] + 5 \sinh^{-1} \left( \frac{9 \ln[\varphi/\Lambda] + 2}{\sqrt{5}} \right). \quad (4.27)$$

The expression for the field at the end of inflation  $\varphi_e$  can be computed from eq. (2.17) by setting  $\mathcal{X} = 1 + 1/\ln(\varphi/\Lambda)$ . At the leading order, we get  $\ln(\varphi_e/\Lambda) \sim 2/\sqrt{3} - 1 \sim 0.15$ , which depends neither on  $\xi$  nor  $\Lambda$ . Applying these results to eq. (4.23), one can see that at leading order,  $n_s$  mainly depends only on the number of e-foldings if  $\xi$  is significantly large.

From our numerical calculation, if  $\xi > 10^4$  and  $\Lambda > 0.1$ , the number of e-foldings has to lie within the range  $30 \lesssim \mathcal{N} \lesssim 60$  satisfying  $n_s$  at  $2\sigma$  CL, i.e.  $0.943 \lesssim n_s \lesssim 0.975$ . The decreasing value of  $\xi$  and  $\Lambda$  tends to enhance those of both  $n_s$  and  $\mathcal{A}_s$ . Hence this can raise the bound on the number of e-foldings if either  $\xi$  or  $\Lambda$  becomes smaller. Recall, however, that  $\xi$  is much larger than unity for this consideration. When  $\xi$  is large,  $|\zeta|^2$  can be expanded as

$$|\zeta|^2 \simeq \frac{(\ln[\varphi/\Lambda])^3(6 \ln[\varphi/\Lambda] + 1)}{\pi^2(6 \ln[\varphi/\Lambda] - 1)\xi^2} + \mathcal{O}(1/\xi^3). \quad (4.28)$$

This equation shows that the power spectrum amplitude depends on the number of e-foldings, and becomes smaller when  $\xi$  is larger. Moreover, one can see that the parameter  $\Lambda$  is weakly constrained by observational bound on the power spectrum amplitude. Only the coupling  $\xi$  can be effectively constrained for this case.

From figure (7), we find that  $\mathcal{A}_s$  gets smaller if  $\mathcal{N}$  is raised, and for the satisfied number of e-foldings, i.e.  $30 \lesssim \mathcal{N} \lesssim 60$ , the observational bound constrains the non-minimal coupling  $\xi$  to be slightly larger than  $3.5 \times 10^4$ . From our numerical calculation, we discover that the amplitude of power spectrum is a decreasing function on  $\xi$ . When  $\xi$  is small, eq. (4.24) shows

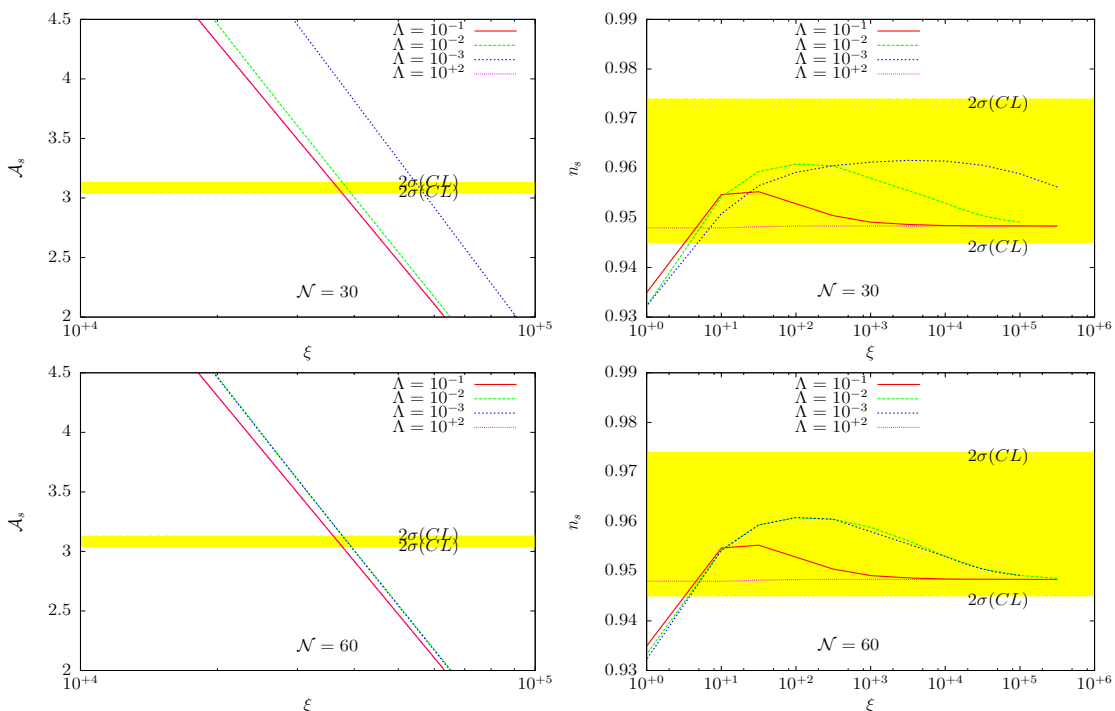


**Figure 7.** The spectral index and amplitude of power spectrum as a function of  $\Lambda$  and  $\xi$  for  $\mathcal{N} \simeq 30$  (top panels) and for  $\mathcal{N} \simeq 60$  (bottom panels). The yellow band corresponds to the  $\pm 2\sigma$  uncertainty.

that the slow-roll evolution of the field requires  $\varphi^2 \gg 1/8$  and  $\varphi^2 \ln(\varphi/\Lambda) \gg 1/32$ . It follows from eq. (4.22) that this conditions can be satisfied when  $n_s \sim 0.96$ , e.g.,  $\varphi^2 \sim 3/0.16$ , and  $\Lambda = 10^{-3}$ . We next check whether the power spectrum amplitude can satisfy the observation

bound when  $\xi$  is small. For small  $\xi$ , we can expand  $|\zeta|^2$  as

$$|\zeta|^2 \simeq \frac{16\varphi^6(\ln[\varphi/\Lambda])^3}{3\pi^2(1+4\ln[\varphi/\Lambda])^2} - \frac{\varphi^6(\ln[\varphi/\Lambda])^2}{3\pi^2(1+4\ln[\varphi/\Lambda])^3} \left[ -1 - 8\ln[\varphi/\Lambda] - 16(\ln[\varphi/\Lambda])^2 + 64\varphi^2(\ln[\varphi/\Lambda])^2 \right] \xi + \mathcal{O}(\xi^2). \quad (4.29)$$

Since during the slow evolution of the inflaton,  $\varphi^2 \gg 1/8$  and  $\varphi^2 \ln(\varphi/\Lambda) \gg 1/32$ , the first term in the above equation gives  $|\zeta|^2 > 10^{-4}$ . This amount of  $|\zeta|^2$  is much larger than  $|\zeta|^2 \sim 10^{-9}$  required by observations. It can be seen that this large contribution to  $|\zeta|^2$  is difficult to be canceled by the second terms in the above equation. This implies that the power spectrum from the glueball model of composite inflation cannot satisfy the observational data for a small  $\xi$ .

In general, the potential arises in this model of composite inflation cannot leads to the realistic inflation, because it becomes negative when  $\varphi < \Lambda$  and its minimum is negative. In the next section, we will consider the other motivation for composite inflation model that leads to the better form of potential for inflation.

### 4.3 Super Yang-Mills Inflation (SYMI)

This model has been explored in [14] in the context of four-dimensional strongly interacting field theories non-minimally coupled to gravity. The authors showed that it is viable to achieve successful inflation driven by orientifold field theories. When the number of colors  $N_c$  is large, such theories feature super Yang-Mills properties. In this investigation, we assign the inflaton as the gluino-ball state in SYM theory. The effective Lagrangian in supersymmetric gluodynamics was constructed in 1982 by Veneziano and Yankielowicz (VY) [24]. The component bosonic form of the VY Lagrangian was summarized in [25].

As always investigated in standard fashion, we take the scalar component part of the super-glueball action and coupled it non-minimally to gravity. Focusing only on the modulus of the inflaton field and introducing the field  $\varphi$  possessing unity canonical dimension and related to  $\Phi$  as  $\Phi = \varphi^3$ , the action of the theory for our investigation is given by

$$\mathcal{S}_{\text{SYMI}} = \int d^4x \sqrt{-g} \left[ \frac{1 + N_c^2 \xi \varphi^2}{2} R - \frac{9N_c^2}{\alpha} g^{\mu\nu} \partial_\mu \varphi \partial_\nu \varphi - V_{\text{SYMI}}(\varphi) \right], \quad (4.30)$$

where

$$V_{\text{SYMI}}(\varphi) = 4\alpha N_c^2 \varphi^4 (\ln[\varphi/\Lambda])^2, \quad (4.31)$$

with  $N_c$  a number of colors. With the action given above, we find

$$F(\varphi) = 1 + N_c^2 \xi \varphi^2 \quad \text{and} \quad G = \frac{18N_c^2}{\alpha}. \quad (4.32)$$

Our analysis hereafter is completely parallel to that of the previous ones. We then plot  $\Delta$ ,  $\mathcal{F}_t$  and  $\epsilon$  in figure (5) and figure (6). From figure (8), we see that for the whole inflation eqs. (2.14) is better approximated by (2.10). Figure (10) shows that the constancy of  $\mathcal{F}_t$  and  $\epsilon$  during initial state of inflation, and the relevant expressions for eq. (2.19) are viable approximations. It is convenient to introduce a set of parameters:

$$X \equiv N_c^2 \xi \varphi^2, \quad Z \equiv 1 + X, \quad W \equiv (3 + \alpha\xi) X, \quad \Sigma_\pm \equiv \alpha\xi (\pm 2 + 3X), \quad (4.33)$$



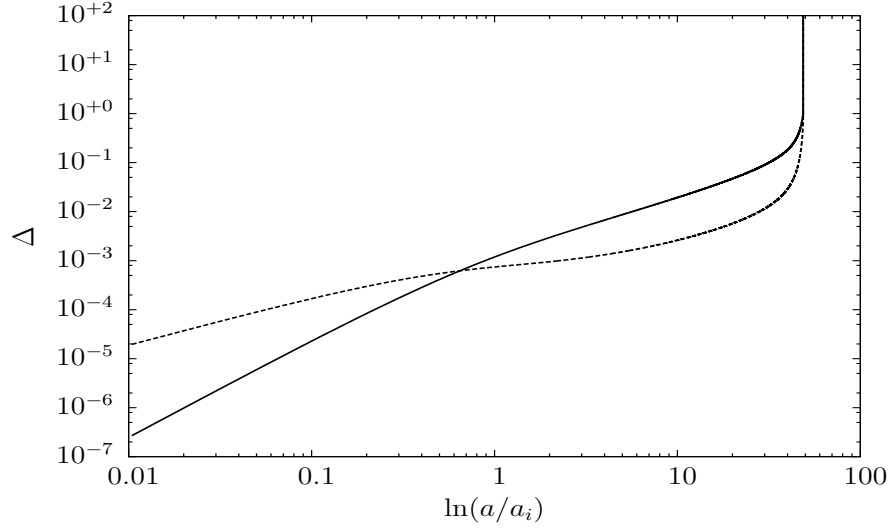


**Figure 8.** The solid line represents the difference between the solutions of eq. (2.14) and eq. (2.10), while the long dashed line represents the difference between the solutions of eq. (2.14) and eq. (3.21). In this plot, we set  $\xi \simeq 10^4$ ,  $\Lambda \simeq 10^{-3}$ ,  $\mathcal{N} = 50$  and  $N_c^2 = 9$ .

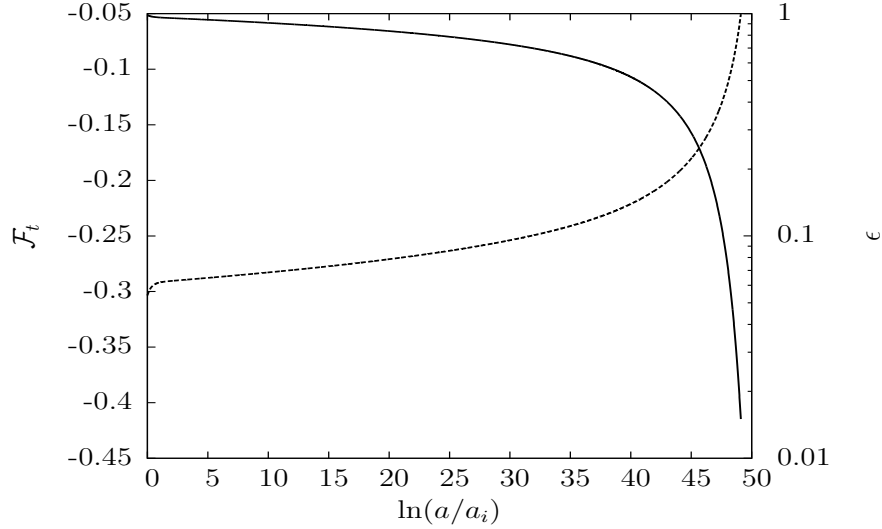


**Figure 9.** The evolution of  $\mathcal{F}_t$  is represented by solid line, while the evolution of  $\epsilon$  is represented by long dashed line. In this plot, we opt  $\xi \simeq 10^4$ ,  $\Lambda \simeq 10^{-3}$ ,  $\mathcal{N} = 50$  and  $N_c^2 = 9$ .

$$U_1 \equiv \alpha^2 \xi^2 X (3 + 2X), \quad V_1 \equiv \alpha \xi Z (17 + 24X), \quad \Psi \equiv 1 + X + 2Y, \quad (4.34)$$

$$U_2 \equiv \alpha^2 \xi^2 X (6 + 7X), \quad V_2 \equiv \alpha \xi Z (4 + 9X), \quad \Gamma \equiv 3 + (3 + \alpha \xi) X, \quad (4.35)$$

$$T_1 \equiv \alpha \xi Z (1 + 2Z (2 + X)), \quad T_2 \equiv \alpha^2 \xi^2 X (1 + 3X (5 + 2X)), \quad (4.36)$$

$$\Theta \equiv 2N^2 \varphi^2 (3 + W) Y, \quad \Xi_{\pm} \equiv \pm \alpha \xi Z + (9 + 9X + \Sigma_{\pm}) Y. \quad (4.37)$$

For this model, eqs. (3.17) and (3.19) can be expressed in terms of the above parameters as follows:

$$n_s = 1 - \frac{1}{[\Theta + \Xi_+^2]} \left[ 7\alpha^2 \xi Z^3 (3 + W) + 6Z^2 (36Z^2 + 2U_1 + V_1)Y + 12Z(45Z^2 + U_2 + 4V_2)Y^2 + 8(27Z^2(3 + 2X) + 18T_1 + T_2)Y^3 \right], \quad (4.38)$$

and

$$|\zeta|^2 = \frac{N_c^4 \varphi^5 \Gamma Y^4 \sqrt{N_c^2 (\alpha \varphi \xi (1 + X) + \varphi (\Xi_+ - \alpha \xi Z))^2}}{2\pi^2 Z^2 \Xi_- \Psi}, \quad (4.39)$$

where the field  $\varphi$  is evaluated at the horizon exit. In this analysis, we deduce  $\varphi > \Lambda$  during inflation. Using  $\xi$ -expansion, we find for  $\xi \rightarrow 0$ :

$$n_s \simeq 1 - \frac{2\alpha (2 + 5Y + 6Y^2)}{9N^2 \varphi^2 Y^2} + \frac{[9\alpha^2 + (38\alpha^2 - 72\alpha N^2 \varphi^2) Y + 64\alpha^2 Y + (48\alpha^2 - 72\alpha N^2 \varphi^2) Y^3]}{162N^2 \varphi^2 Y^3} + \mathcal{O}(\xi^2), \quad (4.40)$$

and for  $\xi \rightarrow \infty$ :

$$n_s \simeq 1 + \frac{7 + 24Y}{2Y(1 + 3Y)^2} - \frac{[7\alpha + (71\alpha - 54N^2 \varphi^2) Y + (240\alpha - 216N^2 \varphi^2) Y^2 + 300\alpha Y^3 + 144\alpha Y^4]}{2\alpha N^2 \varphi^2 Y (1 + 3Y)^3 \xi} + \mathcal{O}\left(\frac{1}{\xi^2}\right). \quad (4.41)$$

In order to determine the magnitude of the field  $\varphi$  during inflation, we write eq.(2.10) for this model in the small  $\xi$  and large  $\xi$  respectively as

$$\begin{aligned} \frac{\varphi'}{\varphi} &\simeq -\frac{\alpha}{9N_c^2 \varphi^2} \left[ 2 + \frac{1}{\ln[\varphi/\Lambda]} \right] \\ &+ \frac{\alpha \xi}{81N_c^2 \varphi^2 (\ln[\varphi/\Lambda])^2} \left[ \alpha + (4\alpha - 9N_c^2 \varphi^2) \ln[\varphi/\Lambda] + 4\alpha (\ln[\varphi/\Lambda])^2 \right] \\ &+ \mathcal{O}(\xi^2), \end{aligned} \quad (4.42)$$

and and

$$\begin{aligned} \frac{\varphi'}{\varphi} &\simeq \frac{1}{2} \left[ -3 - \frac{2}{\ln[\varphi/\Lambda]} + \frac{1}{\ln[\varphi/\Lambda]} \sqrt{(4 + 8 \ln[\varphi/\Lambda] + 9(\ln[\varphi/\Lambda])^2)} \right] \\ &- \frac{1}{2N_c^4 \xi \varphi^2} \left[ 4N_c^2 + \frac{9N_c^4 \varphi^2}{\alpha} + \frac{2N_c^2}{\ln[\varphi/\Lambda]} \right. \\ &\quad \left. - \frac{N_c^6 \varphi^2 (4\alpha + 10\alpha \ln[\varphi/\Lambda] + (8\alpha + 27N_c^2 \varphi^2) (\ln[\varphi/\Lambda])^2)}{\alpha \ln[\varphi/\Lambda] \sqrt{N_c^8 \varphi^4 (4 + 8 \ln[\varphi/\Lambda] + 9(\ln[\varphi/\Lambda])^2)}} + \frac{9}{\alpha \ln[\varphi/\Lambda]} \right. \\ &\quad \left. \left[ -3N_c^4 \varphi^2 \ln[\varphi/\Lambda] - 2N_c^4 \varphi^2 + \sqrt{N_c^8 \varphi^2 (4 + 8 \ln[\varphi/\Lambda] + 9(\ln[\varphi/\Lambda])^2)} \right] \right] \\ &+ \mathcal{O}(1/\xi^2). \end{aligned} \quad (4.43)$$

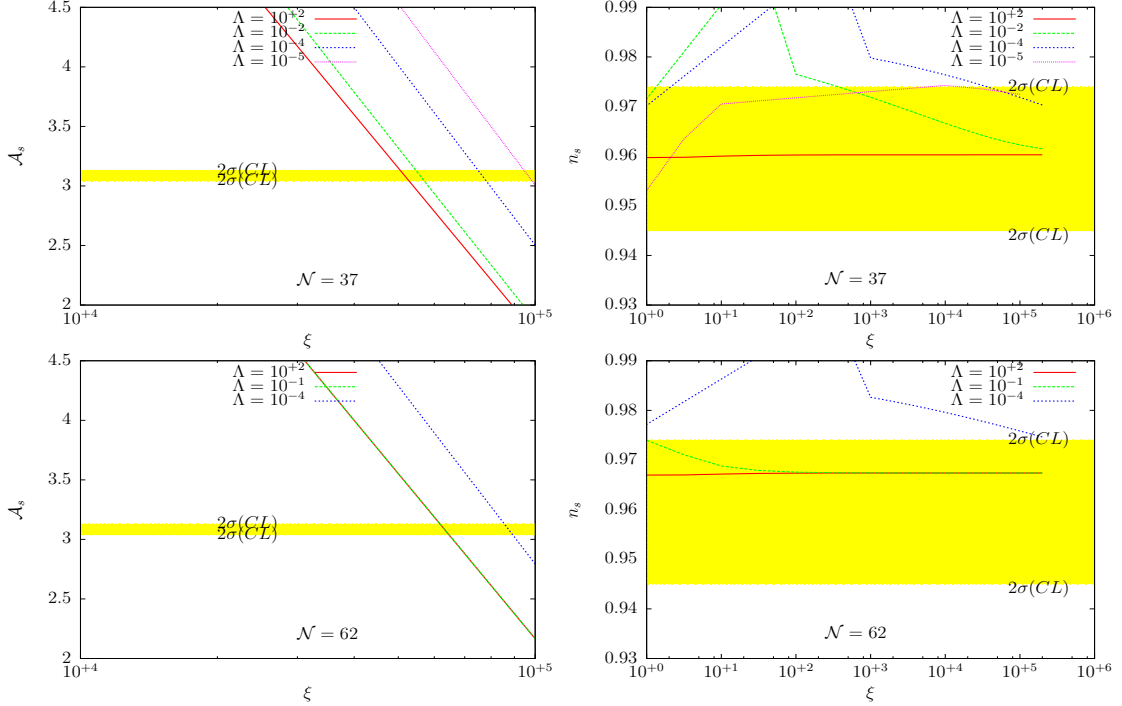


**Figure 10.** The spectral index and amplitude of power spectrum as a function of  $\Lambda$  and  $\xi$  for  $\mathcal{N} \simeq 37$  (top panels) and for  $\mathcal{N} \simeq 62$  (bottom panels). The yellow band corresponds to the  $\pm 2\sigma$  uncertainty.

For a large coupling, eq.(4.43) yields the slow-roll evolution of the field roughly constrained to be  $\ln[\varphi/\Lambda] \gg 1$ . It follows from eq. (4.41) that if  $\xi$  is significantly large,  $n_s$  will mainly depend on  $\ln(\varphi/\Lambda)$  only. Using the leading contributions to  $\varphi'/\varphi$  from eq. (4.43), one can write the number of e-foldings in terms of  $\ln(\varphi/\Lambda)$  via

$$\mathcal{N} \simeq \mathcal{N}(\varphi) - \mathcal{N}(\varphi_e), \quad (4.44)$$

where

$$108\mathcal{N}(\varphi) \equiv 81(\ln[\varphi/\Lambda])^2 + (12 + 27 \ln[\varphi/\Lambda]) \sqrt{9(\ln[\varphi/\Lambda])^2 + 8 \ln[\varphi/\Lambda] + 4} + 108 \ln[\varphi/\Lambda] + 20 \sinh^{-1} \left( \frac{9 \ln[\varphi/\Lambda] + 4}{2\sqrt{5}} \right). \quad (4.45)$$

The expression for  $\varphi_e$  in this case can be estimated from eq. (2.17) by setting  $\mathcal{X} = 1 + 2/\ln(\varphi_e/\Lambda)$ . At leading order, we get  $\ln(\varphi_e/\Lambda) \sim 0.3$  which is independent of  $\xi$  and  $\Lambda$ . This implies that for significantly large  $\xi$ ,  $n_s$  depends only on the number of e-foldings.

From our numerical calculation, if  $\xi > 10^4$  and  $\Lambda > 0.1$ , the number of e-foldings has to lie within the range  $37 \lesssim \mathcal{N} \lesssim 80$  satisfying  $n_s$  at  $2\sigma$  CL. Contrary to the gluball model, the observational bound on the number of e-foldings gets smaller affecting from the reduction of  $\xi$  and  $\Lambda$ . This is so since the amplitude of power spectrum will increase associated with an increasing value of  $\mathcal{N}$ . When  $\xi$  is large, eq. (4.39) can be expanded as

$$|\zeta|^2 \simeq \frac{Y^4 [3Y + 1]}{2\pi^2 N_c^2 [3Y - 1] \xi^2} + \mathcal{O}(1/\xi^3). \quad (4.46)$$

It follows from the above relation that the observational bound on power spectrum amplitude can be used to constrain the coupling  $\xi$ . From our numerical calculation presented in figure (10), we discover that the amplitude of power spectrum becomes larger if either  $\mathcal{N}$  increases,  $\xi$  decreases or when  $\Lambda$  decreases below 0.1 so that  $\xi \gtrsim 5 \times 10^4$  and  $\Lambda > 10^{-5}$  providing the  $n_s$  and  $\mathcal{A}_s$  satisfies the observational bound at  $2\sigma$  CL. For a small coupling  $\xi$ , eq.(4.42) yields the slow-roll evolution of the field naively constrained to be  $\varphi^2 \gg 2\alpha/9N_c^2$  and  $\varphi^2 \ln[\varphi/\Lambda] \gg \alpha/9N_c^2$ . At leading order, eq. (4.40) yields  $n_s \sim 1 - |\varphi'/\varphi|$ , so that  $n_s$  can satisfy the observational bound if  $|\varphi'/\varphi| \sim \mathcal{O}(10^{-3})$ . In the small  $\xi$  limit,  $|\zeta|^2$  from eq. (4.39) can be expanded as

$$|\zeta|^2 \simeq \frac{3N_c^4 \varphi^6 Y^4}{2\pi^2 (1+2Y)^2} - \frac{N_c^4 \varphi^6 Y^3}{6\pi^2 (1+2Y)^3} \left[ \left( -2\alpha - 8\alpha Y + 27N_c^2 \varphi^2 Y - 8\alpha Y^2 + 18N_c^2 \varphi^2 Y^2 \right) \right] \xi + \mathcal{O}(\xi^2). \quad (4.47)$$

From this equation, we see that  $|\zeta|^2$  will be of the order of  $10^{-9}$  as required by observation if  $N_c^4 \varphi^6 Y^4 \ll (1+Y)^2$ . Nevertheless, during inflation, the conditions  $\varphi^2 \gg 2\alpha/9N_c^2$  and  $\varphi^2 \ln[\varphi/\Lambda] \gg \alpha/9N_c^2$  for the slow evolution of inflaton is required. Hence,  $|\zeta|^2$  can be order of  $10^{-9}$  if  $Y^2/(N_c^2(1+2Y)^2)$  is significantly small. This ratio can be small if  $\varphi \gtrsim \Lambda$  or  $N_c^2 \gg 1$ . Since  $\varphi = \Lambda$  at the minimum of the potential, during inflation it is difficult for  $\varphi$  to get close to  $\Lambda$  such that  $Y \ll 1$ . In order to satisfy the observational bound on the power spectrum amplitude,  $N_c^2$  has to be unacceptable large if  $\Lambda < 1$ . For example, from numerical calculation, if we set the number of e-folding equals to 60,  $\xi = 10^{-2}$  and  $\Lambda = 10^{-3}$ , we will get  $n_s = 0.95$ , and will get  $|\zeta|^2 \sim 10^{-9}$  if  $N_c^2 > 10^{10}$ . In the same manner as the previous section for glueball-inspired paradigm, for a small coupling, it is difficult for  $|\zeta|^2$  to be fitted in the observational bound at  $\mathcal{O}(10^{-9})$ .

## 5 Conclusions

In this work, we constrain the model parameters of various composite inflation models using the observational bound for the scalar spectrum index  $n_s$  and amplitude of power spectrum of the primordial curvature perturbations from Planck data. In order to satisfy the observational constraints, the general action for the composite inflation has to be in the form of scalar-tensor theory, such that the inflaton is non-minimally coupled to gravity. We compute the power spectrum for the curvature perturbations by supposing that the slow-roll parameter  $\epsilon$  and the ratio  $\mathcal{F}_t = F_\Phi \varphi' / (2F)$  are approximately constant during the early stage of inflation in which the interesting perturbations modes exit the horizon. Both the analytic expressions and numerical value for  $n_s$  and the power spectrum amplitude  $\mathcal{A}_s$  are calculated.

According to our analytical analysis, we can show that  $n_s$  and  $\mathcal{A}_s$  for the Techni-Inflation can satisfy the observational data for a wide range of the inflaton self-coupling  $\kappa$  when an appropriate value of  $\xi$  is chosen. When  $\xi$  is large,  $n_s$  solely depends on the number of e-foldings. Moreover, the amplitude of the power spectrum depends on the ratio  $\kappa/\xi^2$ , so that we can constrain  $\kappa$  for any appropriate value of the coupling  $\xi$  matching with recent investigation for single field model non-minimally coupled to gravity [16]. However, we find, for a small coupling  $\xi$ , one can constrain the self-coupling  $\kappa$ . From the numerical calculation, the value of  $n_s$  and  $|\zeta|^2$  will lie within the observational bound up to  $1\sigma$  (CL) if the number of e-foldings lie between 43 and 62, and  $\kappa/\xi^2 \sim \mathcal{O}(10^6)$  for a large coupling. Moreover, we discover that in order to satisfy the observational bound  $\kappa > 10^{-14}$  for  $\mathcal{N} \simeq 55$ .

For composite inflationary models from pure and super Yang-Mills theories, we show analytically that  $n_s$  and  $|\zeta|^2$  can satisfy the observational bound if  $\xi$  is significantly large. Similar to the Techni-Inflation,  $n_s$  depends only on  $\mathcal{N}$  when  $\xi$  is large and  $\Lambda$  is not too small. At leading order for a large  $\xi$  limit,  $\mathcal{A}_s$  depends only on  $\mathcal{N}$  and  $\xi$ . Both  $n_s$  and  $\mathcal{A}_s$  are weakly sensitive to the scale  $\Lambda$  if and only if  $\Lambda > 0.1$ . From the numerical results for the glueball model, we discover that  $30 \lesssim \mathcal{N} \lesssim 60$  to obtain  $0.943 \lesssim n_s \lesssim 0.975$ , and for this range of  $\mathcal{N}$ , the  $\xi$  is constrained to be larger than  $3.5 \times 10^4$  for  $3.04 \lesssim \mathcal{A}_s \lesssim 3.13$ . Finally, for the super Yang-Mills model, the numerical investigation yields  $0.943 \lesssim n_s \lesssim 0.975$  for  $37 \lesssim \mathcal{N} \lesssim 80$ . In addition, the power spectrum amplitude can be satisfied the observational bound if the coupling  $\xi \gtrsim 5 \times 10^4$  and  $\Lambda > 10^{-5}$ .

## Acknowledgement

P.C. has just left the Department of Physics at the Faculty of Liberal Arts and Science (FLAS), Kasetsart University, Kamphaeng Saen Campus. There is no way to acknowledge all FLAS's staff members, or even any of them properly. P.C. was truly and deeply indebted to Ms. Wilai Jangboon, Dr. Suntree Sangjan and Mr. Wadchara Thongsamer for their incredible hospitality during his time in Nakhon Pathom. K.K. is supported by Thailand Research Fund (TRF) through grant RSA5480009.

## References

- [1] A. A. Starobinsky, Phys. Lett. B **91**, 99 (1980).
- [2] K. Sato, Mon. Not. R. Astron. Soc. **195**, 467 (1981).
- [3] K. Sato, "Cosmological baryon-number domain structure and the first order phase transition of a vacuum", Phys. Lett. **99B**, 66 (1981).
- [4] D. Kazanas, "Dynamics Of The Universe And Spontaneous Symmetry Breaking," Astrophys. J. **241** L59 (1980).
- [5] A. H. Guth, "The Inflationary Universe: A Possible Solution To The Horizon And Flatness Problems," Phys. Rev. D **23**, 347 (1981).
- [6] A. D. Linde, "A New Inflationary Universe Scenario: A Possible Solution of the Horizon, Flatness, Homogeneity, Isotropy and Primordial Monopole Problems," Phys. Lett. B **108**, 389 (1982)
- [7] A. Albrecht and P. J. Steinhardt, "Cosmology for Grand Unified Theories with Radiatively Induced Symmetry Breaking," Phys. Rev. Lett. **48**, 1220 (1982).
- [8] A. D. Linde, "Chaotic Inflation," Phys. Lett. B **129**, 177 (1983).
- [9] K. Freese, J. A. Frieman and A. V. Olinto, "Natural inflation with pseudo - Nambu-Goldstone bosons," Phys. Rev. Lett. **65**, 3233 (1990).
- [10] F. C. Adams, J. R. Bond, K. Freese, J. A. Frieman and A. V. Olinto, "Natural inflation: Particle physics models, power law spectra for large scale structure, and constraints from COBE," Phys. Rev. D **47**, 426 (1993) [hep-ph/9207245].
- [11] A. D. Linde, Phys. Rev. D **49**, 748 (1994) [astro-ph/9307002].
- [12] P. Channuie, J. J. Joergensen and F. Sannino, "Minimal Composite Inflation," JCAP **1105**, 007 (2011) [arXiv:1102.2898 [hep-ph]].
- [13] F. Bezrukov, P. Channuie, J. J. Joergensen and F. Sannino, "Composite Inflation Setup and Glueball Inflation," Phys. Rev. D **86**, 063513 (2012) [arXiv:1112.4054 [hep-ph]].

- [14] P. Channuie, J. J. Jorgensen and F. Sannino, “Composite Inflation from Super Yang-Mills, Orientifold and One-Flavor QCD,” *Phys. Rev. D* **86**, 125035 (2012) [arXiv:1209.6362 [hep-ph]].
- [15] P. A. R. Ade *et al.* [Planck Collaboration], “Planck 2013 results. XXII. Constraints on inflation,” arXiv:1303.5082 [astro-ph.CO].
- [16] S. Tsujikawa, J. Ohashi, S. Kuroyanagi and A. De Felice, *Phys. Rev. D* **88**, 023529 (2013) [arXiv:1305.3044 [astro-ph.CO]].
- [17] A. Riotto, “Inflation and the theory of cosmological perturbations,” hep-ph/0210162.
- [18] T. Qiu and K. -C. Yang, “Non-Gaussianities of Single Field Inflation with Non-minimal Coupling,” *Phys. Rev. D* **83**, 084022 (2011) [arXiv:1012.1697 [hep-th]].
- [19] T. Kobayashi, M. Yamaguchi and J. 'i. Yokoyama, “Generalized G-inflation: Inflation with the most general second-order field equations,” *Prog. Theor. Phys.* **126**, 511 (2011) [arXiv:1105.5723 [hep-th]].
- [20] F. Sannino and K. Tuominen, “Orientifold theory dynamics and symmetry breaking,” *Phys. Rev. D* **71**, 051901 (2005) [hep-ph/0405209].
- [21] D. K. Hong, S. D. H. Hsu and F. Sannino, “Composite Higgs from higher representations,” *Phys. Lett. B* **597**, 89 (2004) [hep-ph/0406200].
- [22] D. D. Dietrich, F. Sannino and K. Tuominen, “Light composite Higgs and precision electroweak measurements on the Z resonance: An Update,” *Phys. Rev. D* **73**, 037701 (2006) [hep-ph/0510217].
- [23] D. D. Dietrich, F. Sannino and K. Tuominen, “Light composite Higgs from higher representations versus electroweak precision measurements: Predictions for CERN LHC,” *Phys. Rev. D* **72**, 055001 (2005) [hep-ph/0505059].
- [24] G. Veneziano and S. Yankielowicz, “An effective lagrangian for the pure N = 1 supersymmetric Yang-Mills theory”, *Phys. Lett. B* **113**, 3 (1982)
- [25] F. Sannino and M. Shifman, “Effective Lagrangians for orientifold theories,” *Phys. Rev. D* **69**, 125004 (2004) [hep-th/0309252].
- [26] M. Cvetič, T. Hubsch, J. C. Pati and H. Stremnitzer, “A Natural Origin Of Inflation Within A Class Of Supersymmetric Preon Models,” *Phys. Rev. D* **40**, 1311 (1989).
- [27] S. D. Thomas, “Moduli inflation from dynamical supersymmetry breaking,” *Phys. Lett. B* **351**, 424 (1995) [hep-th/9503113].
- [28] J. Garcia-Bellido, “Dual inflation,” *Phys. Lett. B* **418**, 252 (1998) [hep-th/9707059].
- [29] R. Allahverdi, K. Enqvist, J. Garcia-Bellido and A. Mazumdar, “Gauge invariant MSSM inflaton,” *Phys. Rev. Lett.* **97**, 191304 (2006) [hep-ph/0605035].
- [30] K. Hamaguchi, K. -I. Izawa and H. Nakajima, “Supersymmetric Inflation of Dynamical Origin,” *Phys. Lett. B* **662**, 208 (2008) [arXiv:0801.2204 [hep-ph]].
- [31] N. Evans, J. French and K. -y. Kim, “Holography of a Composite Inflaton,” *JHEP* **1011**, 145 (2010) [arXiv:1009.5678 [hep-th]].
- [32] G. L. Alberghi and R. Casadio, “Non-Gaussianity from Compositeness,” arXiv:1010.4395 [astro-ph.CO].
- [33] G. L. Alberghi, “CMB: A Look Inside the Inflaton,” arXiv:0902.4787 [gr-qc].